The Theoretical Description for Amavadin-Ion Electrochemical Determination in *Amanita muscaria* Mushroom Pulp and Extract by Galvanostatic Conducting Polymer Doping

Volodymyr V. Tkach [1,2,*] [iD], **Marta V. Kushnir** [1] [iD], **Vira V. Kopiika** [3] [iD], **Olga V. Luganska** [3] [iD], **Lyudmyla O. Omelyanchik** [3] [iD], **Zholt O. Kormosh** [4] [iD], **Mariia P. Mytchenok** [5] [iD], **Jarem R. Garcia** [6] [iD], **Karina V. Palamarek** [7] [iD], **Konon L. Bagrii** [7] [iD], **Oksana P. Vitriak** [8] [iD], **Anzhelika O. Medvedeva** [8] [iD], **Sílvio C. De Oliveira** [2] [iD], **Petro I. Yagodynets** [iD] [1,*] **Dilafruz B. Razhabova** [9] [iD], **Laziz N. Niyazov** [9] [iD], **Dilfuza M. Musayeva** [9] [iD], **Xayriddin Kosimov** [9] [iD], **Oysha Jabborova** [9] [iD], **Bakhodirjon Samadov** [9] [iD], **Gulandom Sagdullayeva** [9] [iD], **Gulhayo Hamdanova** [8] [iD], **Viktoriia V. Payentko** [10] [iD], **Eugeny M. Demianenko** [10] [iD], **José Inácio Ferrão da Paiva Martins** [11] [iD], **Lucinda Vaz dos Reis** [12] [iD]

1   Chernivtsi National University, 58000, Kotsyubyns´ky Str. 2, Chernivtsi, Ukraine
2   Mato Grosso do Sul Federal University, Av. Sen. Felinto. Müller, 1555, C/P. 549, 79074-460, Campo Grande, MS, Brazil
3   Zaporizhzhia National University, 69600, Zhukovsky Str. 66, Zaporizhzhia, Ukraine
4   Eastern European National University, 43000, Voli Ave., 13, Lutsk, Ukraine
5   Bukovinian State Medical University, 58001, Teatralna Sq., 9, Chernivtsi Ukraine
6   Ponta Grossa State University, Campus de Uvaranas, Av. Gal. Carlos Cavalcanti, 4748, 84030-900, Ponta Grossa, PR, Brazil
7   Chernivtsi Institute of Trade and Economics of Kyiv National University of Trade and Economics, 58012, Central Sq. 9, Chernivtsi, Ukraine
8   Kyiv National University of Trade and Economics, 02156, Kyoto Str. 21, Kyiv, Ukraine
9   Abu Ali Ibn Sino Bukhara State Medical Institute, 705018, Navoi Str., 1, Bukhara, Uzbekistan
10 Chuiko Institute of Surface Chemistry of National Academy of Science of Ukraine, 03164, Gen. Naumov Str. 17, Kyiv, Ukraine
11 Engineering Faculty of the University of Porto, 4200-465, Rua Dr. Roberto Frias, s/n, Porto, Portugal
12 University of Trás-os-Montes and Alto Douro, Quinta de Prados, 5001-801, Folhadela, Vila Real, Portugal
*   Correspondence: nightwatcher2401@gmail.com (V.V.T.); ved1988mid@rambler.ru (P.I.Y.)

Abstract: The theoretical description for amavadin-ion electrochemical determination in mushroom pulp has been given for the first time. The correspondent mathematical model has been developed and analyzed by linear stability theory and bifurcation analysis, providing the theoretical investigation of the electrochemical behavior of the electroanalytical system. It has been shown that the system behavior in galvanostatic mode is more dynamic than in potentiostatic mode, which is reflected in the enhancement of the probability of the electrochemical oscillations due to the intense influence of chemical and electrochemical stages on both DEL and surface charge. Nevertheless, the system is efficient for electroanalysis or conducting polymer modification for electroanalytical purposes.

Keywords: *Amanita muscaria*; amavadin-ion; conducting polymers; electrochemical sensors; stable steady-state.

1. Introduction

Amavadin [1 – 4] (Figure 1) is an ion naturally found in fly agaric (*A. muscaria*) mushrooms. It is a vanadium-based complex present in the mushroom in both reduced and oxidized forms. The exact function of the ion in the mushroom organism has not been determined yet, but it has already been known that it acts as an oxidant in mushroom skin.
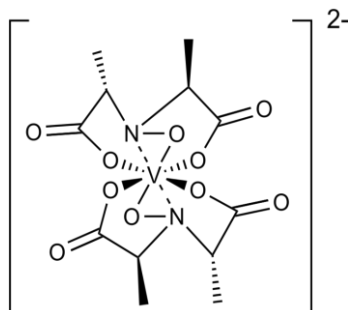
Figure 1. Amavadin-ion structure.

Being a redox-active compound of natural origin, amavadin is interesting as a green electrode modifier for either conducting polymer or carbon material electrodes [5 – 10] in electroanalytics, as it is suitable for anodic doping. Moreover, two forms, corresponding to tetra- and pentavalent vanadium, are highly toxic to human organisms (toxic effects include diarrhea, vomiting, glomerulonephritis, and pyelonephritis), as most of the vanadium compounds [11 – 15], the reason why its determination becomes highly actual. By this, the conducting polymer doping may be efficiently used for electroanalytical purposes, for amavadin concentration, or polymer electrode modification.

Nevertheless, the possibility of electrochemical instabilities, observed in similar systems with the electrosynthesis and modification of conducting polymers, including the electroanalytical systems [16 – 18], is very important in the theoretical analysis of this system in order to pose this process in practice. Therefore, this work aims to analyze, from the theoretical point of view, the system's behavior with conducting polymer amavadin-doping for electroanalysis and electrode modification in galvanostatic mode. By this, the correspondent model will be developed and analyzed by means of linear stability theory and bifurcation analysis, and the system's behavior will be thereby compared to that of similar electroanalytical systems involving ionic and non-ionic systems [19 – 21].

2. System and its Modeling

Taking into account the electrochemical behavior of neutral conducting polymer in galvanostatic mode, we may conclude that in the first stage, the tetravalent amavadin enters the polymer matrix, thereby being oxidized in the second stage. The analytical signal, by this, maybe either potentio- or conductometric.

Taking this into account, we introduce three variables:

a – amavadin concentration in the pre-surface layer;
p – amavadin-doped conducting polymer surface coverage degree;
q – the electrode charge density.

Assuming some suppositions [20, 21], we describe the behavior of this system by the trivariant equation-set, expressed as (1):

$$\begin{cases} \frac{da}{dt} = \frac{2}{\delta}\left(\frac{\Delta}{\delta}(a_0 - a) - r_d\right) \\ \frac{dp}{dt} = \frac{1}{P}(r_d - r_o) \\ \frac{dq}{dt} = i - i_F \end{cases} \qquad (1)$$

in which Δ is the diffusion coefficient, P is the doped polymer maximal surface concentration, i_F is the Faradaic current, a_0 is the amavadin bulk concentration, and the parameters r are the correspondent reaction rates, calculated as $(2-3)$.

$$r_d = k_d a(1-p)\exp\left(\frac{nF\varphi_0}{RT}\right) \qquad (2)$$

$$r_o = k_o p \exp\left(\frac{F\varphi_0}{RT}\right) \qquad (3)$$

As for the Faradaic current, it is calculated as (4):

$$i_F = nF k_d a(1-p)\exp\left(\frac{nF\varphi_0}{RT}\right) + F k_o p \exp\left(\frac{F\varphi_0}{RT}\right) \qquad (4)$$

in which the parameters k stand for the correspondent reaction rate constants, n is the number of electrons transferred during the doping, F is the Faraday number, R stands for the universal gas constant, and T is the absolute temperature.

Taking into account the additional factors valid for galvanostatic mode, the oscillatory behavior in this system will be more probable than for potentiostatic mode and other similar systems [20, 21]. Nevertheless, this process is efficient from both electroanalytical and electrosynthetical points of view, as shown below.

3. Results and Discussion

In order to investigate the behavior of the system with the electrochemical doping of neutral conducting polymer by amavadin-ion, we analyze the equation-set (1), taking into account the algebraic relations $(2-4)$ through linear stability theory. The steady-state Jacobian matrix members will be described as:

$$\begin{pmatrix} a_{11} & a_{12} & a_{13} \\ a_{21} & a_{22} & a_{23} \\ a_{31} & a_{32} & a_{33} \end{pmatrix} \qquad (5)$$

Herein:

$$a_{11} = \frac{2}{\delta}\left(-\frac{\Delta}{\delta} - k_d(1-p)\exp\left(\frac{nF\varphi_0}{RT}\right)\right) \qquad (6)$$

$$a_{12} = \frac{2}{\delta}\left(k_d a \exp\left(\frac{nF\varphi_0}{RT}\right) - j k_d a(1-p)\exp\left(\frac{nF\varphi_0}{RT}\right)\right) \qquad (7)$$

$$a_{13} = \frac{2}{\delta}\left(-l k_d a(1-p)\exp\left(\frac{nF\varphi_0}{RT}\right)\right) \qquad (8)$$

$$a_{21} = \frac{1}{P}\left(k_d(1-p)\exp\left(\frac{nF\varphi_0}{RT}\right)\right) \qquad (9)$$

$$a_{22} = \frac{1}{P}\left(-k_d a \exp\left(\frac{nF\varphi_0}{RT}\right) + j k_d a(1-p)\exp\left(\frac{nF\varphi_0}{RT}\right) - k_o \exp\left(\frac{F\varphi_0}{RT}\right) + j k_o p \exp\left(\frac{F\varphi_0}{RT}\right)\right) \qquad (10)$$

$$a_{23} = \frac{1}{P}\left(l k_d a(1-p)\exp\left(\frac{nF\varphi_0}{RT}\right) + l k_o p \exp\left(\frac{F\varphi_0}{RT}\right)\right) \qquad (11)$$

$$a_{31} = -nF k_d(1-p)\exp\left(\frac{nF\varphi_0}{RT}\right) \qquad (12)$$

$$a_{32} = -nF\left(-k_d a \exp\left(\frac{nF\varphi_0}{RT}\right) + j k_d a(1-p)\exp\left(\frac{nF\varphi_0}{RT}\right)\right) - F\left(k_o \exp\left(\frac{F\varphi_0}{RT}\right) - j k_o p \exp\left(\frac{F\varphi_0}{RT}\right)\right) \qquad (13)$$

$$a_{33} = nF\left(l k_d a(1-p)\exp\left(\frac{nF\varphi_0}{RT}\right)\right) + F\left(l k_o p \exp\left(\frac{F\varphi_0}{RT}\right)\right) \qquad (14)$$

Taking into account the main diagonal elements (6), (10), and (14), we conclude that the oscillatory behavior in this system is more probable than in similar systems [20, 21] either due to the influence of both of the electrochemical stages on DEL electrophyslcal properties or due to the more dynamic nature of galvanostatic processes, while compared to potentiostatic.

The oscillatory behavior may be possible if the Hopf bifurcation conditions are satisfied. The necessary condition for its realization is the presence of the positive elements (responsible for the positive callback) in the Jacobian main diagonal. These elements are: $jk_d a(1-p) \exp\left(\frac{nF\varphi_0}{RT}\right)$ and $jk_o p \exp\left(\frac{F\varphi_0}{RT}\right)$ if j>0, like also $nF\left(lk_d a(1-p) \exp\left(\frac{nF\varphi_0}{RT}\right)\right) + F\left(lk_o p \exp\left(\frac{F\varphi_0}{RT}\right)\right) > 0$, if l>0. The oscillatory behavior is explained by the cyclic changes of both electrochemical stages on the electrophysical properties of DEL and surface, as well as the electrode charge density. The cyclic influences are generated by the conducting polymer doping and the dopant oxidation with changes in dopant charge and charge density distribution. Either way, the oscillation frequency will highly depend on the background electrolyte composition, including the pH.

As for the steady-state stability, its topological region will be slightly narrower than for the simplest case due to more dynamic behavior in galvanostatic mode. In order to facilitate the stability analysis by the Routh-Hurwitz criterion, we introduce new variables and rewrite the determinant as (15):

$$\frac{4F}{\delta^2 P}\begin{vmatrix} -\kappa - \Xi & \Lambda & -P \\ \Xi & -\Lambda - \Omega & P + T \\ -n\Xi & n\Lambda + \Omega & nP + T \end{vmatrix} \quad (15)$$

which, according to the determinant properties, will be rewritten as (16):

$$\frac{4F}{\delta^2 P}\begin{vmatrix} -\kappa - \Xi & \Lambda & -P \\ \Xi & -\Lambda - \Omega & P + T \\ 0 & -(n-1)\Omega & 2nP + (n+1)T \end{vmatrix} \quad (16)$$

Applying the Det J<0 condition, salient from the criterion, opening the straight brackets, and changing the signs, we obtain the stability requirement, expressed as (17):

$$\kappa\big((n-1)\Omega(P+T) - (\Lambda+\Omega)(2nP + (n+1)T)\big) + \Xi\big((n-1)\Omega T - (2\Lambda+\Omega)(2nP + 2(n+1)T)\big) > 0 \quad (17)$$

This condition describes the mostly kinetically controlled electroanalytically efficient system, although its topological satisfaction region will be slightly narrower than for the potentiostatic mode, but even though it will remain efficient from both electroanalytical and electrosynthetical points of view, as it is readily satisfied, if the DEL parameters j and l are negative or, even being positive, have small positive values. Really, if j and l are negative, the kinetic parameters P and T become negative, and the kinetic parameters Ω and Λ become positive. By this, the left side of the inequity (17) will be driven towards more positive values, stabilizing the system.

Taking into account that no side reaction capable of compromising the polymer and/or amavadin stability occurs in this system, we conclude that the steady-state stability will correspond to the linear dependence between the concentration and potential, providing an efficient analytical signal interpretation. The conductometric measures also give the possibility to relate the doping degree to the concentration.

As for the detection limit, its condition is correspondent to the monotonic instability and is described as:

$$\kappa\big((n-1)\Omega(P+T)-(\Lambda+\Omega)(2nP+(n+1)T)\big)+\Xi\big((n-1)\Omega T-(2\Lambda+\Omega)(2nP+2(n+1)T)\big)=0 \qquad (18)$$

In the case of the conducting polymer overoxidation, which may accompany the galvanostatic electropolymerization and doping processes, part of the polymer will be transformed into a less conducting form. In most cases, the dopant will leave the polymer matrix, returning to the pre-surface layer. Thus, the model will be rewritten as:

$$\begin{cases} \frac{da}{dt} = \frac{2}{\delta}\left(\frac{\Lambda}{\delta}(a_0 - a) - r_d + r_S\right) \\ \frac{dp}{dt} = \frac{1}{P}(r_d - r_o - r_S) \\ \frac{dq}{dt} = i - i_F \end{cases} \qquad (19)$$

and analyzed in our next works.

4. Conclusions

The system with amavadin galvanostatic electrochemical determination by intercalation into neutral conducting polymer as a dopant has been analyzed from the mechanistic point of view. The analysis of the correspondent model has shown that the system's behavior will be more dynamic than the potentiostatic mode, leading to the more probable oscillatory behavior manifestation. Even though, in galvanostatic mode, the system remains a kinetically controlled electroanalytical efficient process.

Funding

Acknowledgments

Conflicts of Interest

References

1. Housecroft, C.E. The fungus *Amanita Muscaria*. From Neutoroxin to Vanadium Accumulation. *Chimia* **2019,** *73,* 96 – 97, https://doi.org/10.2533/chimia.2019.96.
2. Carboue, Q.; López, M. Amanita muscaria: Ecology, Chemistry, Myths, *Encyclopedia* **2021**, *1*, 905 – 914, https://doi.org/10.3390/encyclopedia1030069.
3. Voynova, M.; Shkondrov, A.; Kondeva-Burdina, M.; Krasteva, I. Toxicological and pharmacological profile of Amanita muscaria (L.) Lam. – a new rising opportunity for biomedicine. *Pharmacia* **2020,** *67,* 317 – 323, https://doi.org/10.3897/pharmacia.67.e56112.
4. Braeuer, S.; Walenta, M.; Steiner, L.; Goessler, W. Determination of the naturally occurring vanadium complex amavadin in Amanita muscaria with HPLC-ICPMS. *J. Anal. Atom Spectroscop.* **2021,** *36*, 954 – 967, https://doi.org/10.1039/D0JA00518E.
5. de Oliveira, R.W.S.; Barros Gomes, P.R.; Diniz Ribeiro, J.; Batista Reis, J.; Alves Fontenele, M.; Oliveira Everton, G.; da Silva Lyra, W.; Costa Louzeiro, H.; do Livramento de Paula, M.; Mouchrek Filho, V.E. Determinação Espectrofotométrica de Cobre (II) em Aguardente de Mandioca (Tiquira). *Rev. Colomb. Cien. Quím. Farm.* **2020**, *49*, 353 – 371, https://doi.org/10.15446/rcciquifa.v49n2.89507 (in Portuguese).

6. Joshi, N.C.; Malik, S.; Gururani, P. Utilization of Polypyrrole/ZnO Nanocomposite in the Adsorptive Removal of Cu [2+], Pb [2+] and Cd [2+] Ions from Wastewater. *Letters in Applied NanoBioScience* **2021**, *10*, 2339–2351, https://doi.org/10.33263/LIANBS103.23392351.

7. Ramanavicius, S.; Morkvenaite-Vilkonciene, I; Samukaite-Bubniene, U.; Ratautaitė, V.; Plikusienė, I.; Viter, R.; Ramanavičius, A. Electrochemically Deposited Molecularly Imprinted Polymer-Based Sensors. *Sensors* **2022,** *22*, 1282, https://doi.org/10.3390/s22031282.

8. Akkapinyo, Ch.; Subannajui, K; Poo-arporn, Y.; Poo-arporn, R.P. Disposable Electrochemical Sensor for Food Colorants Detection by Reduced Graphene Oxide and Methionine Film Modified Screen Printed Carbon Electrode. *Molecules* **2021,** *26*, 2312, https://doi.org/10.3390/molecules26082312.

9. Monnappa, A.B.; Manjunatha, J.G.G.; Bhatt, A.S.; Nagarajappa, H. Sensitive and Selective Electrochemical Detection of Vanillin at Graphene Based Poly(Methyl Orange) Modified Paste Electrode. *J. Sci. Adv. Mat. Dev.* **2021,** https://doi.org/10.1016/j.jsamd.2021.05.002.

10. Thadathil, A.; Pradeep, H.; Joshy, D.; Ismail, Y.A.; Periyat, P. Polyindole and Polypyrrole as a Sustainable Platform for Environmental Remediation and Sensor Applications. *Mater Adv.* **2022,** *3*, 2990 – 3022, https://doi.org/10.1039/D2MA00022A.

11. Chiarelli, R.; Martino, C; Roccheri, M.C; Geraci, F. Vanadium Toxicity Monitored by Fertilization Outcomes and Metal Related Proteolytic Activities in Paracentrous Lividus Embryos. *Toxics* **2022,** *10*, 83, https://doi.org/10.3390/toxics10020083.

12. Waidyanatha, S.; Weber, F.X.; Fallacara, D.M.; Harrington, J.M.; Levine, K.; Robinson, V.G.; Sparrow, B.R.; Stout, M.D.; Fernando, R.; Hooth, M.J.; Xie, G.; Roberts, G.K. Systemic Exposure and Urinary Excretion of Vanadium Following Perinatal Subchronic Exposure to Vanadyl Sulfate and Sodium Metavanadate via Drinking Water. *Toxicol. Lett.* **2022,** *360*, 53 – 61, https://doi.org/10.1016/j.toxlet.2022.03.004.

13. Shireen, F.; Nawaz, M.A.; Lu, J.; Xiong, M.; Kaleem, M.; Huang, Y.; Bie, Z. Application of Boron Reduces Vanadium Toxicity by Altering the Subcellular Distribution of Vanadium, Enhancing Boron Uptake and Enhancing the Antioxidant Defense System of Watermelon. *Ecotoxicol. Env. Safety* **2021,** *226*, 112828, https://doi.org/10.1016/j.ecoenv.2021.112828.

14. Das, S.; Roy, A.; Barui, A.K.; Alabbasi, M.M.A.; Kuncha, M.; Sistla, R.; Sreedhar, B.; Patra, C.R. Anti-Angiogenic Vanadium Pentoxide Nanoparticles for the Treatment of Melanoma and Their *in vivo* Toxicity Study. *Nanoscale* **2020,** *12*, 7604 – 7621, https://doi.org/10.1039/D0NR00631A.

15. Kovalevski, V.V; Moshnikov, I.A. Vanadium Carbides in Shungite. *Eur. J. Mineral.* **2022,** *34*, 131 – 141, https://doi.org/10.5194/ejm-34-131-2022.

16. Das, I.; Goel, N.; Agrawal, N.R.; Gupta, S.K. Growth Patterns of Dendrimers and Electric Potential Oscillations during Electropolymerization of Pyrrole using Mono- and Mixed Surfactants. *The Journal of Physical Chemistry B* **2010**, *114*, 12888-12896, https://doi.org/10.1021/jp105183q.

17. Das, I.; Goel, N.; Gupta, S.K.; Agrawal, N.R. Electropolymerization of pyrrole: Dendrimers, nano-sized patterns and oscillations in potential in presence of aromatic and aliphatic surfactants. *Journal of Electroanalytical Chemistry* **2012**, *670*, 1-10, https://doi.org/10.1016/j.jelechem.2012.01.023.

18. Aoki, K.; Mukoyama, I.; Chen, J. Competition between Polymerization and Dissolution of Poly(3-methylthiophene) Films. *Russian Journal of Electrochemistry* **2004**, *40*, 280-285, https://doi.org/10.1023/B:RUEL.0000019665.59805.4c.

19. Tkach, V.V.; Kushnir, M.V.; Omelchenko, N.M.; Rogozynsky, M.S.; de Oliveira, S.C.; Stotoshchuk, N.M.; Yagodynets, P.I. The Theoretical Description for Amavadin Electrochemical Determination by Poly(Vedelolactone) Doping. *Appl. J. Env. Eng. Sci.* **2019,** *5*, 384 – 389, https://doi.org/10.48422/IMIST.PRSM/ajees-v5i4.15374.

20. Tkach, V.V.; Kushnir, M.V.; de Oliveira, S.C.; Parchenko, V.V.; Odyntsova, V.M.; Aksyonova, I.I.; Ivanushko, Y.G.; Yagodynets, P.I.; Kormosh, Z.O. A Descrição Matemática Da Detecção Eletroquímica da Ergina, Assistida Pelos Novos Derivados Triazólicos, Dopados pelo Íon Amavadina. *Rev. Colomb. Cien. Quím. Farm.* **2021,** *50,* 174 – 184, https://doi.org/10.15446/rcciquifa.v50n1.95451 (in Portuguese).

21. Tkach, V.; Kushnir, M.; de Oliveira, S.; Ivanushko, Y.; Tkach, V.; Mytrofanova, H.; Zadoia, A.; Yagodynets', P.; Kormosh, Z.; Luganska, O. Theoretical Description for an Efficient Rhenium Electrocatalytical Recuperation by Polypyrrole Overoxidation. *Letters in Applied NanoBioScience* **2021**, *10*, 2396-2401, https://doi.org/10.33263/LIANBS103.23962401.